Comparison of Beyond Standard Model Signatures in the Fully Hadronic $t\bar{t} + E_{\mathrm{T}}^{\mathrm{miss}}$ Channel

Mathew Fraser Robertson, University of Glasgow, United Kingdom

September 11, 2018

Abstract

Previous searches for dark matter, supersymmetry, and dark energy at the LHC have been carried out independently. However, due to the likeness in experimental signatures of these models there are going to be joint searches in the fully hadronic $t\bar{t} + E_{\mathrm{T}}^{\mathrm{miss}}$ channel. This study compared the main experimental signatures of WIMP dark matter, effective scalar field dark energy and supersymmetry on a plane of $< p_{\mathrm{T}}^{t1,2} >$ and $< E_{\mathrm{T}}^{\mathrm{miss}} >$ to aid in the design of signal regions for these searches. The study found that 2-body decays from direct stop production with an $m_{\tilde{t}}$, $m_{\tilde{\chi}}$ split of 300 GeV had a similar signature to WIMP dark matter with a pseudo-scalar mediator. In addition, it also found that 3- and 4-body decays from direct stop production radiated significantly more than the other supersymmetry and WIMP dark matter models. Different behaviour was observed for dark energy depending on the chosen effective operator.

Contents

1 Introduction

The quantum field theory describing the fundamental building blocks of the universe and their interactions (excluding gravity of course) has long been coined the Standard Model (SM) of particle physics. Despite its strong predictive ability, there are clear experimental and theoretical challenges that plague SM. As such, extensions are needed for the theory to become compatible with observations, giving rise to Beyond Standard Model (BSM) physics.

Supersymmentry (SUSY) is one such model [1, 2]. Large top quark loop corrections to the mass of the Higgs Boson should place it on the Planck scale, however its mass has been measured by ATLAS and CMS at the Large Hadron Collider (LHC) at CERN to be on the GeV scale [3]. This is part of the gauge hierarchy problem - only by extreme fine tuning can the corrections be cancelled, invoking the far from satisfactory implication of grand intelligent design. SUSY offers a much more viable solution by way of introducing massive supersymmetric to each of the fundamental particles in SM. The "superpartner" of the top quark, the top squark, cancels these quantum corrections to within the scale we observe [4].

Gravitational rotation curves, one example in the left panel of Figure 1, show that almost all of the galaxies we observe are spinning faster than their luminous mass should allow. The calculated gravitational potential of these systems is not enough to support the velocity at which they are rotating, hence the stars should be thrown out due to the centripetal forces. This suggests that there exists a substantial amount of unobservable mass - dark matter (DM). Independent observations from gravitational lensing, the cosmic microwave background, and others strongly affirm this. There are several candidates for DM; Weakly interacting Massive Particles (WIMPs), axions, primordial black holes, among others. However due to the "WIMP miracle", the revelation in which particles with the general proerties of the WIMP - weakly interacting and massive - theoretically generate dark matter with the same relic abundance as is observed [5], they are hence the preferred model for DM.

The final BSM physics considered here is concerning dark energy (DE). Before 1998, it was expected that the expansion of space should be decelerating due to the persisting gravitational attraction of matter (including dark matter). However, it was then discovered by observations of Type 1a supernovae that the rate of expansion of space appears to be accelerating [8, 9]. The latest supernovae and baryon acoustic oscillation observations, shown in right panel of Figure 1, are still in agreement with this view point. New physics is thus needed to describe the mechanism opposing gravity, and currently - some 20 years later - there still exists no favourable explanation.

1.1 BSM through $t\bar{t} + E_{\mathbf{T}}^{\mathbf{miss}}$

For WIMPs, assuming that the mediator connecting them to SM particles is Yakawa-like, the coupling strength then scales with mass. As such, the most promising channel to search for these particles is through the most massive SM particle, the top quark. This can be done at the LHC with the ATLAS detector. More specifically, they can be

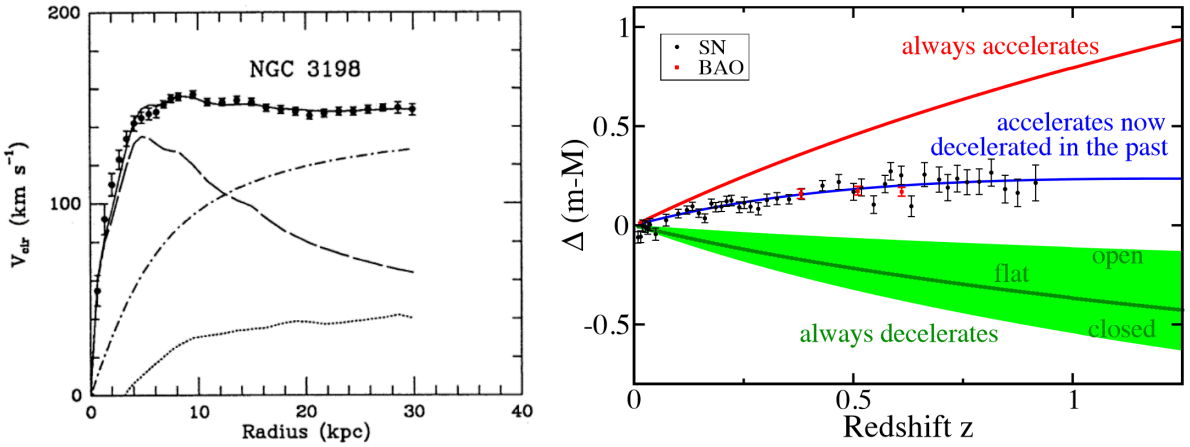

Figure 1: Left: A galaxy rotation curve taken from [6] in which the expected rotation from the luminous matter is demonstrated by the dashed curve and the dot dash curves shows the additional "dark" matter required to maintain the velocity. The dotted curve shows the contribution from dust. Right: This plot taken from [7] fits the current Type 1a supernovae and baryon acoustic oscillation data to different accelerating universe models.

searched for in the $t\bar{t}+E_{\mathrm{T}}^{\mathrm{miss}}$ channel. These are events in which a top, anti-top pair are produced along with the signature of high missing transverse energy, $E_{\mathrm{T}}^{\mathrm{miss}}$, as defined by

$$E_{\mathrm{T}}^{\mathrm{miss}} = -\sum_{i} \vec{p}_{\mathrm{T}}^{\,i} \tag{1}$$

A non-zero $E_{\mathrm{T}}^{\mathrm{miss}}$ implies that there was energy from the event that evaded the detectors - it was missed. Neutrinos are the only SM particle that can leave (or "not leave") such a signature, however other effects such as detector inefficiencies, acceptance range, pileup, etc. can also mimic missing energy. If DM were to be produced in an interaction with tops, then it would not leave a trace in the detectors and thus would have a high $E_{\mathrm{T}}^{\mathrm{miss}}$ signature.
Some Effective Field Theories (EFT) for DE predict something similar, $t\bar{t}$ events in which DE particles are produced leaving no trace in the detector. Similarly, different SUSY events also fall into this channel in which the final deacy products are neutralinos that also behave the same way. Specific details of these models and their decay chains looked at in this analysis can be found in Section 2.

1.2 Project Goals

BSM searches in the at the LHC in the fully hadronic $t\bar{t}+E_{\mathrm{T}}^{\mathrm{miss}}$ channel for DM, DE, and SUSY have previously been carried out separately. However, the experimental signatures for the different models are very similar; high $E_{\mathrm{T}}^{\mathrm{miss}}$ and high p_{T}^{t}. Thus,

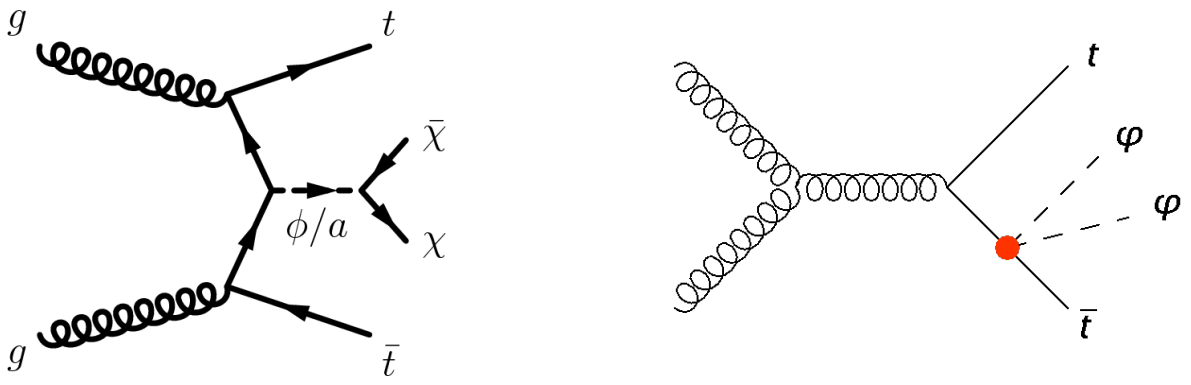

Figure 2: Left: General WIMP dark mater, χ, produced from $t\bar{t}$ events through a Yakawa-like mediator ϕ (or ϕ/a). Figure taken from [10]. Right: Dark energy production in $t\bar{t}$ events in which the corresponding interaction shown in red is unresolvable, figure taken from [11].

the separate groups carrying out these searches are joining forces, and to design signal regions sensitive to all of the different models considered an understanding of how they relate to each other is needed. Hence, a comparison of their characteristic signatures on a $< E_{\mathrm{T}}^{\mathrm{miss}} >$, $< p_{\mathrm{T}}^{t1,2} >$ plane would show which models can be searched for in certain regions. The aim of this project was to produce this plane for general WIMP, SUSY and EFT DE models sensitive to the fully hadronic $t\bar{t} + E_{\mathrm{T}}^{\mathrm{miss}}$ channel at truth level. Specifically, the goals were to create these signature planes for:

- an unbiased selection of events at truth level
- a standard pre-selection similar to previous DM and SUSY selections at truth level
- modified selections corresponding to current and future searches at truth level

2 Models

For WIMPs, only events in which a colour-neutral spin-0 mediator, ϕ, is produced along with a top, t, anti-top, $\bar{t}$, as shown in the left panel of Figure 2 were considered. The mediator then decays into a pair of WIMPs, χ and $\bar{\chi}$, and they contribute the missing energy. The mass of the DM particles was assumed to be $m_{\chi} = 1GeV$ throughout the analysis, while m_{ϕ} was included for a range between 10 - 300 GeV. Both scalar and pseudo-scalar mediators were also compared in the study.
A general EFT - described in detail here [12] - was considered for this analysis. The right panel of Figure 2 shows an effective interaction associated with a $t\bar{t}$ event in which 2 DE particles, ϕ, are produced in the final state. Two types of effective operators were considered for this model; the first, $\mathcal{L}_1$, scales with the mass of the SM particle to which DE couples to (in this case m_t), the second, $\mathcal{L}_2$, scales with the momenta of the SM particles. General EFTs are useful to consider as the incorporate many of the mainstream scalar field models of dark energy without any bias.

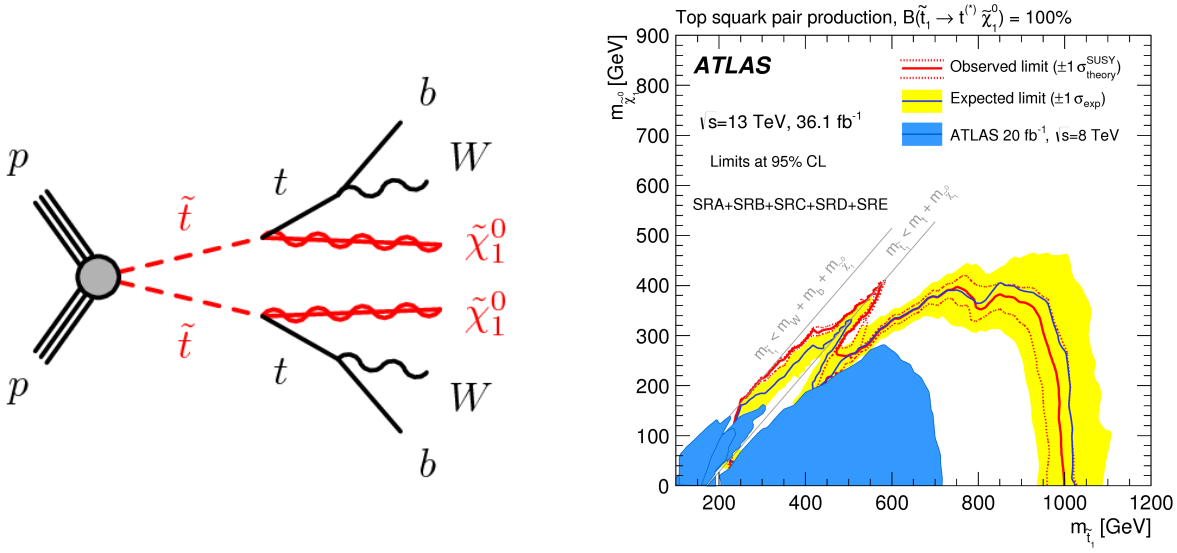

Figure 3: Left: Direct top squark production in which the stops decay to a top quark and a neutralino, $\widetilde{\chi}_1^0$. Right: Exclusion contour for the stop masses, $m_{\widetilde{t}}$, and neutralino masses, $m_{\widetilde{\chi}}$. All mass combinations within the red line have been excluded. Both figures taken from [14].

Four types of SUSY production in association with tops were used in the analysis. The first, shown in the left panel of Figure 3, is for direct stop pair production in which each decay to a top and a neutralino, $\widetilde{\chi}_1^0$.[1], $\widetilde{\chi}_1^0$. The various samples used in the analysis corresponded to varying stop and neutralino masses, $m_{\widetilde{t}}$ and $m_{\widetilde{\chi}}$ respectively, based of the exclusion contour from previous SUSY searches (right panel of Figure 3). There are several interesting regions in the exclusion plane, however only 3 were considered in the study. The first region exists on the right most side of the plane for high $m_{\widetilde{t}}$ and low $m_{\widetilde{\chi}}$. The second, known as the "bulk", looks at smaller mass splitting between the stop and the neutralino. This is just to the left of the first region. The final region is known as the "compressed region", it looks at a very special part of the plane in which the mass splitting exactly the mass of the top quark. Thus, all tops and neutralinos produced in these particular events will gain no kinetic energy from the stop, however the cross-section for such events is very small.
The second and third type of SUSY events used in this analysis were the 3- and 4-body decays from direct stop production shown in Figure 4. In case of 3-body; the stop decays to a b-quark and a chargino, $\widetilde{\chi}_1^{\pm}$, where the chargino decays to a W and a $\widetilde{\chi}_1^0$. 4-body decays are where the stop decays to a b, $\widetilde{\chi}_1^0$, and 2 leptons. These are not $t\bar{t}$ events, however for this study the decay products that were not $\widetilde{\chi}_1^0$'s were considered to be the 'tops'. The mass splittings considered for the 3-body events were between the two grey lines in the right panel of Figure 3, and again about the exclusion contour. The 4-body mass splittings are to the left of the grey lines.
The second SUSY signal model considered in this study was the indirect production of

[1] $\widetilde{\chi}_1^0$ is the lightest stable supersymmetric particle, and is also a candidate for DM [13].

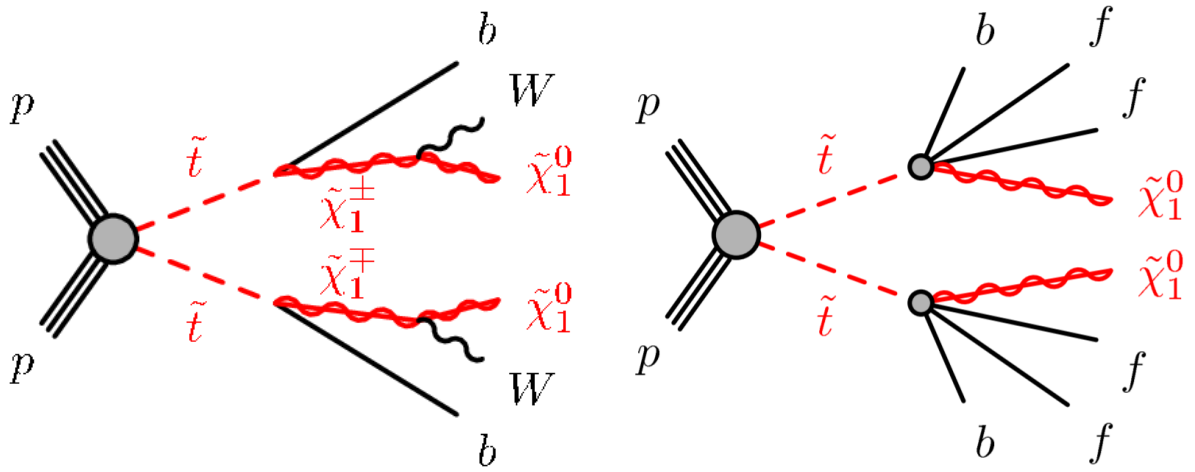

Figure 4: Left: 3-body direct stop production. Stop decays to a chargino, $\widetilde{\chi}_1^{\pm}$ and a b-quark, in which the chargino decays to a W and a neutralino, $\widetilde{\chi}_1^0$. Diagram from [14]. Right: 4-body direct stop production. Stop decays to a neutralino, $\widetilde{\chi}_1^0$, a b-quark and 2 leptons (here labelled f). Diagram taken from [15].

stops from gluino, $\widetilde{g}$, decays - shown in Figure 5. Only one mass splitting was considered here and that was for $m_{\widetilde{g}} = 1700$ GeV and $m_{\widetilde{t}} = 400$ GeV. The mass splitting between the stop and the neutralino in this case was taken to be small (5 GeV) so that the other decay product of the stop was a soft jet.

3 Top Selection

For the analysis retrieving truth top data was vital because the transverse momenta of the top quarks were needed for the plane - the result of the study. However, instead of retrieving data for (maximum) 2 tops, there were sometimes 4 tops present in the events! This, as it turned out, was due to the inclusion the state of the tops before they radiated, and after the radiated. Thus, 4 of them makes perfect sense. It became apparent that they were retrieved in a particular order through analysis of the p_{T}^t for each of the 4 tops and the angular separation between each of them, ΔR;

$$\Delta R = \sqrt{\Delta\phi^2 + \Delta\eta^2} \tag{2}$$

for

$$\eta \equiv \ln\left[\tan\left(\frac{\theta}{2}\right)\right] \tag{3}$$

where η is the pseudo-rapidity and θ is the angle between the particle (jet) and the beam axis.

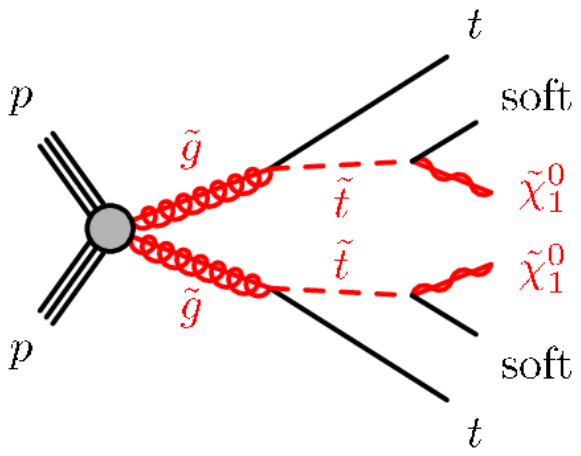

Figure 5: Indirect stop pair production from gluino decays in which top quarks are also produced. The stop pair then decay to neutralinos and soft jets (due to the small selected mass splitting between stop and neutralinos for these events). Figure taken from [14].

Hence, determination of 2 distinct tops for the 4 retrieval case was trivial. It is also important to note that for this analysis only tops after radiation - in their "final state" - were considered.
The expected ΔR distribution for 2 correctly identified top quarks should peak around π due to most top pairs being produced back to back. Left panel of Figure 6 shows this smooth distribution for the case of 4 top retrieval with a clear peak around 3.

3.1 Non-Trivial Top Selection

For the cases where there was not 4 tops retrieved from the event the selection process was not so trivial. It was declared that all top quarks retrieved must have $|\eta| < 2.8$. Beyond this the particles go out of range from the ATLAS detectors acceptance. It was also required that $p_{\mathrm{T}}^{t} > 20$ GeV as below this the top jets are too soft to reconstruct. So tops that either fall into the category of being too soft, or out the reach of acceptance, are not retrieved. This complication meant that if less than 4 tops were recovered from an event, the order in which they were retrieved was rendered meaningless. For case in which either 0 or 1 top was retrieved the event was immediately discarded, there needed to be 2 tops for the analysis.

3.1.1 2 Top Retrieval

For the case of retrieving only 2 tops, the method behind determining whether or not they are separate distinct quarks or not was relatively simple. If the angular separation, ΔR, between the 2 tops is too small it is most likely the same quark, and that the small separation is due to the push from radiating. If the separation is large then - unless the

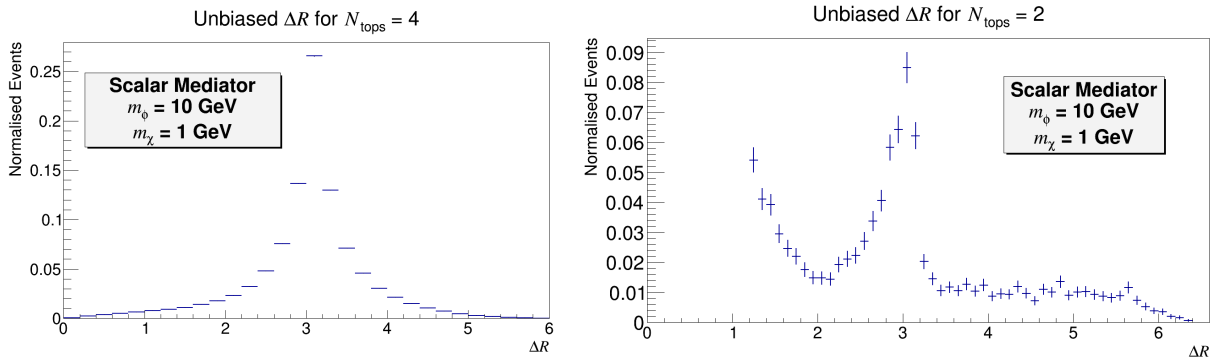

Figure 6: Both plots show the distributions of the angular separation between the two selected top quarks for DM with a scalar mediator of mass 10GeV. Left: For the case of 4 top retrieval at truth level; showing even distribution about π as expected. Right: For the case of 2 top retrieval at truth level; distribution does pek at π, however also peaks towards low separation implying incorrect top selection.

quark has undergone extremely hard radiation - they should be 2 distinct tops. The ΔR distribution for tops that pass a $\Delta R > 1.2$ cut is shown in the right panel of Figure 6. Unlike the 4 top retrieval, left panel of Figure 6, the distribution is not smooth and although there is a peak about 3, there is also a clear peak towards $\Delta R \to 0$. As this makes up only 0.3% of the total events these events were simply discarded[2]. It is interesting to note that 16% of all all events have 2 top retrieval, with the vast majority of these failing to pass the $\Delta R > 1.2$ cut.

3.1.2 3 Top Retrieval

The case of 3 top retrieval is more complicated. Again, the selection of the distinct quarks was carried out by comparing ΔR between each of the 3 tops. If all of them had $\Delta R > 1.2$, then all 3 tops are spread apart and it become difficult to distinguish between them. If more than one $\Delta R < 1.2$ is found then they are all too close together to select the correct tops. Hence, only the specific case where one $\Delta R < 1.2$ is found between 2 of the 3, can we assume that this is because they are indeed the same quark. The ΔR distribution for this case is shown in the left panel of Figure 7, and again a clear peak about 3 with a smooth distribution. Hence, these events were kept in the analysis along with the 4 top retrieval despite only making up about 4% of the total events. Thus, overall between 81-83% of events were able to be saved via this top selection, and the final ΔR distribution for all saved events is shown in the right panel of Figure 7.

[2]All of the statistics and figures in this section are for a scalar DM sample with $m_\phi = 10$ GeV. The methods were also tested on other samples as well.

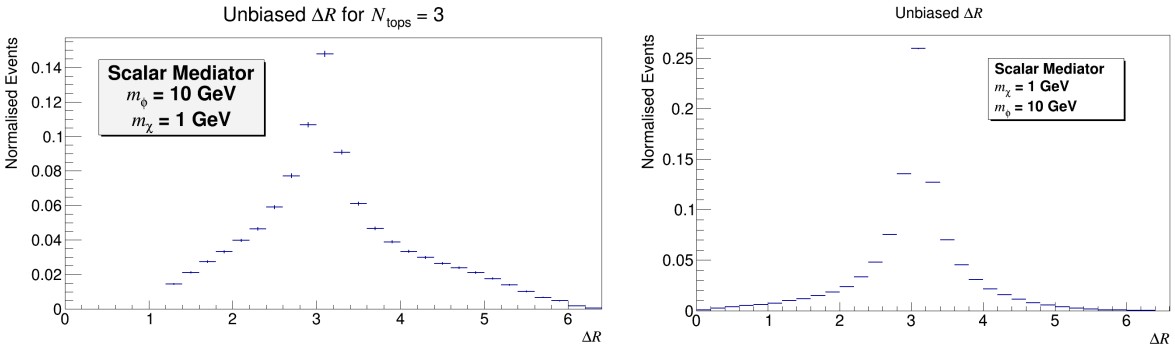

Figure 7: Both plots show the distributions of the angular separation between the two selected top quarks for DM with a scalar mediator of mass 10GeV. Left: For the case of 3 top retrieval at truth level; smooth distribution about π. Right: For all tops that the pass top selection; again a smooth distribution peaking at π.

4 Pre-Selections

For a complete comparison of the different models it is important to understand how the different event selections will impact on the experimental signatures, and what these impacts mean in relation to each model. For this analysis, 4 main pre-selections were applied to the samples:

- 0 lepton requirement only
- Standard pre-selection taken from previous DM and SUSY searches
- Standard pre-selection except with a relaxed $E_{\mathrm{T}}^{\mathrm{miss}}$ requirement
- Standard pre-selection with additional $m_{\mathrm{T}}^{b,\,\mathrm{min}}$ requirement

4.1 Unbiased Selection

The unbiased selection has 1 requirement; 0 leptons. Here, the definition of a lepton is either an electron or a muon, tau leptons were not included in this veto due to the current difficulty in tau reconstruction. An unbiased selection is useful as it allows one to observe how specific cuts impact (bias) the experimental signatures of the different models by giving an insight before any cuts are made.

4.2 Standard Pre-Selection

The main cuts that bias the experimental signatures were applied here:

- 0 lepton requirement
- $E_{\mathrm{T}}^{\mathrm{miss}} > 250$ GeV

- At least 4 jets with $p_{\mathrm{T}} > 80, 80, 40, 40$ GeV
- At least 1 b-tagged jet
- $\Delta\phi_{\mathrm{min}} > 0.4$ between $E_{\mathrm{T}}^{\mathrm{miss}}$ and jets
- Jet cleaning and pileup removal algorithms

Again the 0 lepton requirement was necessary to make sure that it was the fully hadronic channel being analysed. The $E_{\mathrm{T}}^{\mathrm{miss}}$ cut is important as that is what events are triggered on. The requirements on the jets are less important to the signature planes but were included in previous DM and SUSY searches and are hence included here. They essentially help reduce the multi-jet background, this is also the same with the $\Delta\phi_{\mathrm{min}}$ cut. Jet cleaning and pileup removal help mimic experimental accelerator and detector effects but contribute little to the signature planes - again only included as they were in the standard pre-selection.

4.3 Low $E_{\mathrm{T}}^{\mathrm{miss}}$ Pre-Selection

A current issue with DM searches at the LHC is due to the high $E_{\mathrm{T}}^{\mathrm{miss}} > 250$ GeV requirement in the standard pre-selection. Only a minority of DM events actually pass this cut, thus significantly reducing the sensitivity to them. This is demonstrated for DM with a pseudo-scalar mediator in Section 5.1 with Figure 9. However, reducing this cut is problematic. $E_{\mathrm{T}}^{\mathrm{miss}}$ is used as the trigger for these searches and the minimum triggering value is set at 250 GeV for no other reason than the frequency of events needing to be recorded would be too great if it was lowered. Thus, to relax $E_{\mathrm{T}}^{\mathrm{miss}}$ another observable must be used as trigger instead; a team at DESY are currently investigating the use of b-tagging as the trigger to allow a relaxation to of $E_{\mathrm{T}}^{\mathrm{miss}}$. Hence, to follow suit a signature plan with a standard pre-selection except for a relaxation to $E_{\mathrm{T}}^{\mathrm{miss}} > 160$ GeV.

4.4 Standard Pre-Selection + $m_{\mathrm{T}}^{b,\,\mathrm{min}}$

An interesting cut to include is on the transverse mass of between the $E_{\mathrm{T}}^{\mathrm{miss}}$ jet and the closest b-tagged jet, $m_{\mathrm{T}}^{b,\mathrm{min}}$ described by

$$m_{\mathrm{T}}^{b,\mathrm{min}} = \sqrt{p_{\mathrm{T}}^{b,\mathrm{min}} E_{\mathrm{T}}^{\mathrm{miss}} \Big[1 - \cos\Delta\phi\Big(p_{\mathrm{T}}^{b}, p_{\mathrm{T}}^{\mathrm{miss}}\Big)\Big]} \tag{4}$$

A main source of background is picked up from the semi-leptonic decay of a W, in which the lepton is not detected and as the other decay product is a neutrino the event has an $E_{\mathrm{T}}^{\mathrm{miss}}$ signature. Figure 8 demonstrates this scenario. All of the $E_{\mathrm{T}}^{\mathrm{miss}}$ from these events come from the W, and hence are close to the b-jet that decayed from the same top. Thus, the transverse mass of this system has to be less than the mass of the top, m_t. Therefore, a simple cut of $m_{\mathrm{T}}^{b,\mathrm{min}} > m_{\mathrm{top}}$ gets rid of this background.

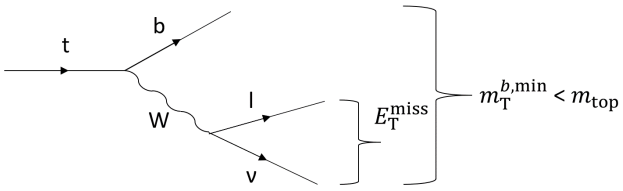

Figure 8: Feynmann diagram for semileptonic top quark decay chain in which the lepton is not picked up by the detectors resulting in an $E_{\mathrm{T}}^{\mathrm{miss}}$ signature. This background must have a transverse mass between the b-jet and the fake $E_{\mathrm{T}}^{\mathrm{miss}}$ "jet" smaller than the mass of top quark.

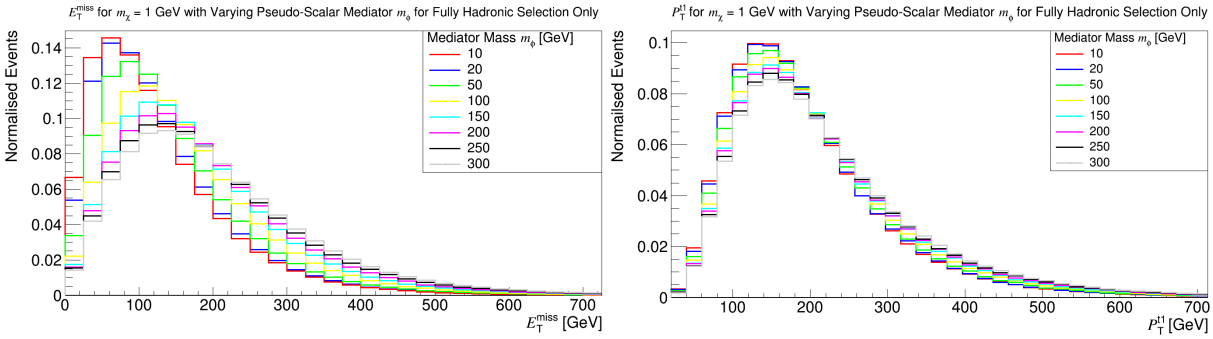

Figure 9: Both plots are for dark matter with a pseudo-scalar mediator of varying mass and the 0 lepton selection only. Left: Missing transverse energy distribution. Right: Distribution of the leading top quark's transverse momentum.

5 DM Observables

5.1 Unbiased

Examples of the change in distribution of observables $E_{\mathrm{T}}^{\mathrm{miss}}$ and p_{T}^{t1} for a pseudo-scalar mediator with changing mass is shown in Figure 9 for an unbiased selection. It is clear that both $E_{\mathrm{T}}^{\mathrm{miss}}$ and p_{T}^{t1} get harder and wider for an increasing m_ϕ. Similar distributions are observed for p_{T}^{t2} and $p_{\mathrm{T}}^{t\bar{t}}$, as well as for scalar mediator DM. These are to be expected as the mediator decays to a constant $m_\chi = 1$ GeV, thus as m_ϕ increases the "excess" energy available to the χ particles should also increase making them more boosted.
An important observation of the peaks in the $E_{\mathrm{T}}^{\mathrm{miss}}$ distributions is that they are all considerably below the value at which the cut $E_{\mathrm{T}}^{\mathrm{miss}} = 250$ Gev is made. In fact, the vast majority of the events are below this cut. As this also applies to the scalar mediator case it thus demonstrates the undesirable inconvenience of the current trigger. It unfortunately has the consequence that searches are only sensitive to events in the tail of the $E_{\mathrm{T}}^{\mathrm{miss}}$ distribution - the minority.

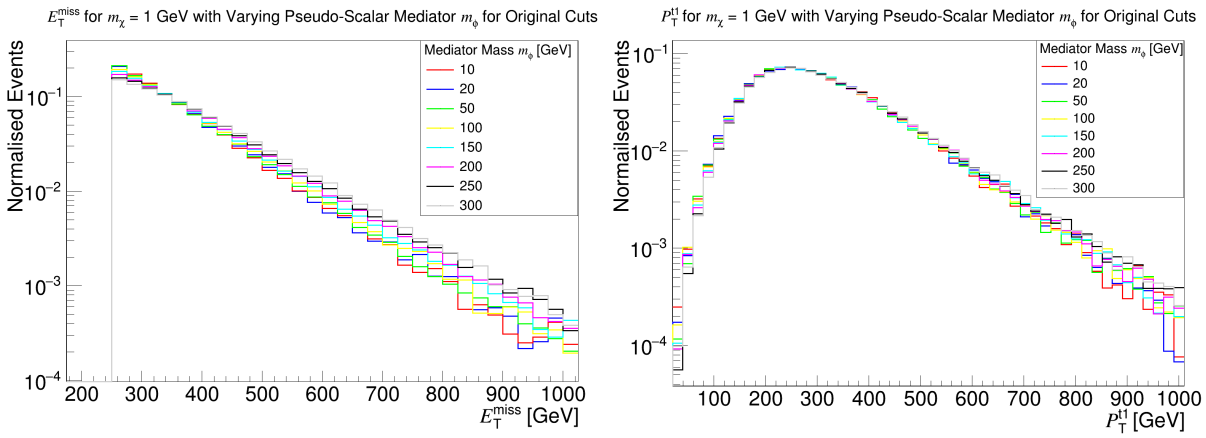

Figure 10: Both plots are for dark matter with a pseudo-scalar mediator of varying mass and the standard pre-selection. Left: Semi-log plot of the missing transverse energy after pre-selection. Right: Distribution of the leading top quark's transverse momentum after pre-selection.

5.2 Biased

The same distributions for the biased selection (standard pre-selection only) are shown in Figure 10. The same trend of harder $E_{\mathrm{T}}^{\mathrm{miss}}$ and p_{T}^{t1} is observed for greater m_ϕ. However, the extend of the boosting is lesser such that a log scale is needed for this to become apparent. Again, this was also observed for p_{T}^{t2} and $p_{\mathrm{T}}^{t\bar{t}}$, as well as for a scalar mediator. The cut flow chart for this selection is shown in figure 11[3]. The efficiency in top selection, described in Section 3, is eveident with a relatively similar small fraction of events lost from process compared to most other cuts. However, the $E_{\mathrm{T}}^{\mathrm{miss}}$ cut makes the biggest impact on the sample causing most of the events to be discarded due to the triggering requirement. I can also be seen that m_{phi} does not have much influence on the extent of each cut with the exception of $E_{\mathrm{T}}^{\mathrm{miss}}$, however this is consistent with the boosted $E_{\mathrm{T}}^{\mathrm{miss}}$ distributions for the unbiased selections shown in the left panel of Figure 9.

6 $< E_{\mathrm{T}}^{\mathrm{miss}} >$ and $< p_{\mathrm{T}}^{t1,2} >$ Planes

6.1 Unbiased and Low $E_{\mathrm{T}}^{\mathrm{miss}}$

The first signature plane, shown in the left panel of Figure 12, is for the 0 lepton only selection and thus represents the unbiased signatures. The DE models were not included in this plane as their samples were generated with a compulsory $E_{\mathrm{T}}^{\mathrm{miss}}$ cut of 150 GeV, and hence were not unbiased. Both the scalar and pseudo-scalar mediator models for DM scale as expected for increasing m_ϕ; both $< E_{\mathrm{T}}^{\mathrm{miss}} >$ and $< p_{\mathrm{T}}^{t1,2} >$ get increase for

[3]It is important to note here that this is the standard pre-selection, hence the $m_{\mathrm{T}}^{b,\mathrm{min}}$ cut is not included despite having a label on the figure.

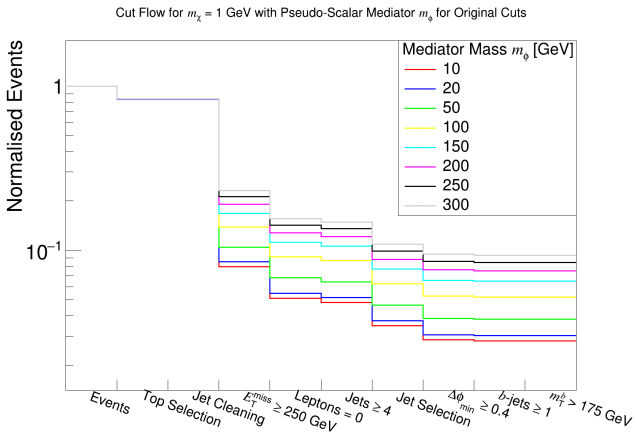

Figure 11: Cut flow plot showing the fraction of events passing the different stages of selection for dark matter with a pseudo-scalar mediator of varying mass.

greater m_ϕ. A similar trend is observed in both direct and indirect SUSY models for increased mass splittings between $m_{\tilde{t}}$ and $m_{\tilde{\chi}}$. The direct stop mass splittings of ($m_{\tilde{t}}$ = 600 [GeV], $m_{\tilde{\chi}}$ = 300 [GeV]), ($m_{\tilde{t}}$ = 700 [GeV], $m_{\tilde{\chi}}$ = 400 [GeV]), and ($m_{\tilde{t}}$ = 800 [GeV], $m_{\tilde{\chi}}$ = 500 [GeV]), matched closely to the scalar DM with high m_ϕ. In particular, ($m_{\tilde{t}}$ = 600 [GeV], $m_{\tilde{\chi}}$ = 300 [GeV]) and scalar m_ϕ = 300 GeV overlap.

The right panel of Figure 12 gives the signature plane for the low $E_{\mathrm{T}}^{\mathrm{miss}}$ selection. The first direct comparison with the unbiased plane that can be drawn is of the significant shift in $< E_{\mathrm{T}}^{\mathrm{miss}} >$ by the DM models due to the $E_{\mathrm{T}}^{\mathrm{miss}} > 160$ GeV requirement. The range of the DM samples also shrink, as well as a shape change for the scalar mediator DM of $m_\phi = 10, 20$ GeV. It is possible that this shape change is due to a phenomena described fully here [16]. The SUSY points on the plane are also shifted to the right, but the points with an unbiased $< E_{\mathrm{T}}^{\mathrm{miss}} >$ greater than 160 GeV were effected less - as would be expected. However, it is interesting to point out that for these specific points their $< p_{\mathrm{T}}^{t1,2} >$ decreases on the low $E_{\mathrm{T}}^{\mathrm{miss}}$ plane. This is contrary to the DM, and low mass splitting SUSY.

The same 3 direct stop SUSY samples that were most closely related to the scalar mediator DM in the unbiased plane - ($m_{\tilde{t}}$ = 600 [GeV], $m_{\tilde{\chi}}$ = 300 [GeV]), ($m_{\tilde{t}}$ = 700 [GeV], $m_{\tilde{\chi}}$ = 400 [GeV]), and ($m_{\tilde{t}}$ = 800 [GeV], $m_{\tilde{\chi}}$ = 500 [GeV]) - now also accompany the pseudo-scalar mediator DM. Comparing the ratio of probabilities of detecting these events between the closest pairs, $P_{\mathrm{SUSY}}/P_{\mathrm{DM}}$, where we define

$$P = \sigma \times \epsilon_{\mathrm{filter}} \times K_{\mathrm{factor}} \times \text{selection efficiency} \tag{5}$$

we find that (($m_{\tilde{t}}$ = 800 [GeV], $m_{\tilde{\chi}}$ = 500 [GeV]) and pseudo-scalar m_ϕ = 300 GeV have a ratio of 0.2, ($m_{\tilde{t}}$ = 600 [GeV], $m_{\tilde{\chi}}$ = 300 [GeV]) and pseudo-scalar m_ϕ = 150 GeV have a ratio of 0.4, and finally ($m_{\tilde{t}}$ = 700, $m_{\tilde{\chi}}$ = 400 [GeV]) lies closest to pseudo-scalar m_ϕ = 250 GeV with a ratio of 0.4. So the probability of detecting these 2-body SUSY models is about 2.5-5 times less likely than for pseudo-scalar mediator DM.

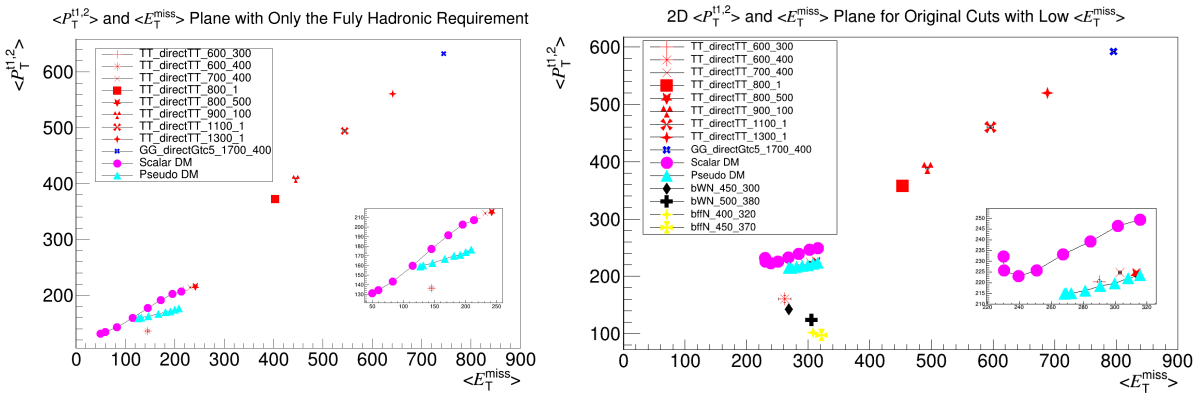

Figure 12: Left: Unbiased signature plane for scalar mediator dark matter in purple balls, pseudo-scalar dark matter in blue triangles, 2-body direct stop production in red and indirect stop production in dark blue. Right: Similar to left plane but with the low missing transverse energy selection, and the inclusion of the 3-body and 4-body direct stop production in black and yellow respectively.

The 3- and 4-body SUSY decays do not lie on the same diagonal as the other models; the $< E_{\mathrm{T}}^{\mathrm{miss}} >$ is noticeably harder than the $< p_{\mathrm{T}}^{t1,2} >$. This shows that these events radiate more after selection than the others. It is also interesting that the ($m_{\tilde{t}} = 600$ [GeV], $m_{\tilde{\chi}} = 400$ [GeV]) 2-body SUSY decay is also in the same region. This particular point is different from the other 2-body SUSY as it has a mass splitting of 200 GeV which is close to the compressed region (mass splitting of 173 GeV). This point is also very close to the 3-body ($m_{\tilde{t}} = 450$ [GeV], $m_{\tilde{\chi}} = 300$ [GeV]) point.

6.2 High $E_{\mathrm{T}}^{\mathrm{miss}}$

The next comparison of planes can be made between the low and high $E_{\mathrm{T}}^{\mathrm{miss}}$ selections. As the cut $E_{\mathrm{T}}^{\mathrm{miss}} > 250$ GeV is sufficiently greater than the generator level cut of 150 GeV for the DE models, they could be included in the high $E_{\mathrm{T}}^{\mathrm{miss}}$ plane[4].. The shift, squish, and shape change of the DM previously discussed for the low $E_{\mathrm{T}}^{\mathrm{miss}}$ plane is even more pronounced for the standard pre-selection. Again, the increased cut has less of an impact on the high mass split SUSY models, however a small shift to increasing $< E_{\mathrm{T}}^{\mathrm{miss}} >$ is observed. The 3 SUSY points that have thus far been close companions to DM appear to have drifted slightly, with a closer relation to the low mass tall of the pseudo-scalar mediator DM. The DE model with effective operator $\mathcal{L}_2$, sensitive to the momenta of the tops, is in a similar region of the signature plane to ($m_{\tilde{t}} = 1100$ [GeV], $m_{\tilde{\chi}} = 1$ [GeV]).

[4]The DE models on these planes were poorly labelled: DE_400 corresponds to model with $\mathcal{L}_1$, and DE_600 corresponds to $\mathcal{L}_2$

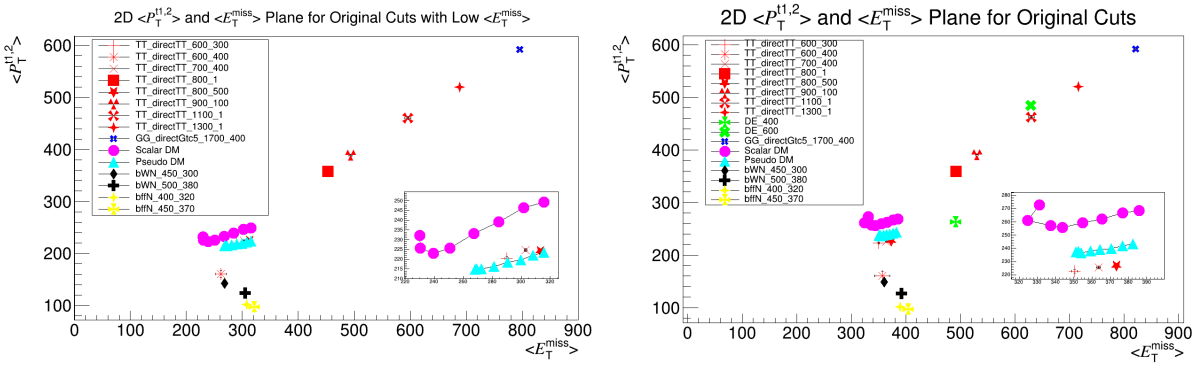

Figure 13: Left: Same plot as the right panel of Figure 12. Right: Signature plane for the high missing transverse energy pre-selection with the inclusion of dark energy in green.

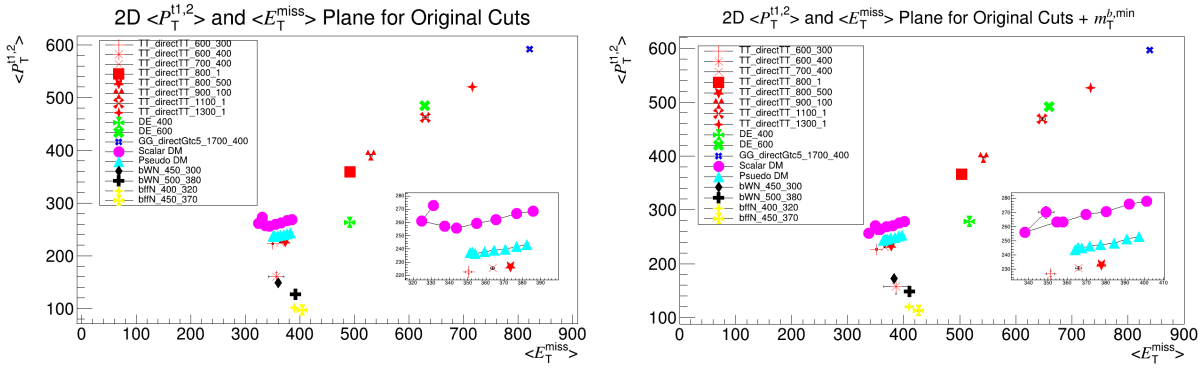

Figure 14: Left: Same plot as the right panel of Figure 13. Right: Signature plane for the high missing transverse energy pre-selection plus the additional cut on the transverse mass .

6.3 High $E_{\mathrm{T}}^{\mathrm{miss}}$ + $m_{\mathrm{T}}^{b,\,\mathrm{min}}$

The final plane to consider is for standard pre-selection with an additional cut on $m_{\mathrm{T}}^{b,\,\mathrm{min}}$, shown in the right panel of Figure 14. This additional cut implemented another shift to higher $< E_{\mathrm{T}}^{\mathrm{miss}} >$ for the DM samples, and also the DE models. This was to be expected from the $E_{\mathrm{T}}^{\mathrm{miss}}$ term in Equation 4 describing $m_{\mathrm{T}}^{b,\mathrm{min}}$. This shift moves the $\mathcal{L}_2$ model slight further away from ($m_{\tilde{t}}$ = 1100 [GeV], $m_{\tilde{\chi}}$ = 1 [GeV]) as it transcends to higher $< E_{\mathrm{T}}^{\mathrm{miss}} >$, however the separation does only vary a little. The 3 SUSY points continue to drift from the pseudo-scalar mediator DM, with the ($m_{\tilde{t}}$ = 600 [GeV], $m_{\tilde{\chi}}$ = 300 [GeV]) model distinctly separate from DM. Both ($m_{\tilde{t}}$ = 700 [GeV], $m_{\tilde{\chi}}$ = 400 [GeV]) and ($m_{\tilde{t}}$ = 800 [GeV], $m_{\tilde{\chi}}$ = 500 [GeV]) remain close to the low m_ϕ pseudo-scalar mediators but with lower $< p_{\mathrm{T}}^{t1,2} >$.

7 Conclusions

For all of the different signature planes considered, there were 3 SUSY models that remained close to the WIMP scalar and pseudo-scalar mediator DM models. These 3 - ($m_{\tilde{t}} = 600$ [GeV], $m_{\tilde{\chi}} = 300$ [GeV]), ($m_{\tilde{t}} = 700$ [GeV], $m_{\tilde{\chi}} = 400$ [GeV]), ($m_{\tilde{t}} = 800$ [GeV], $m_{\tilde{\chi}} = 500$ [GeV]) - all had a mass splitting of 300 GeV and are hence from the bulk region of the $m_{\tilde{t}}$ and $m_{\tilde{\chi}}$ plane. For the 0 lepton condition only, these points sat closest to the scalar mediator of $m_{\phi} = 300$ GeV DM model. For the low $E_{\mathrm{T}}^{\mathrm{miss}}$ plane the points moved to accompany the high mediator mass pseudo-scalar models, and for the high $E_{\mathrm{T}}^{\mathrm{miss}}$ plane it was the same but for the low mass pseudo-scalar mediators. Only with the additional $m_{\mathrm{T}}^{b,\,\mathrm{min}}$ cut was there a noticeable separation between one of the SUSY points, ($m_{\tilde{t}} = 600$ [GeV], $m_{\tilde{\chi}} = 300$ [GeV]) and the pseudo-scalar DM. The cross-sections for these SUSY points were found to be 2.5-5 times smaller than that of the corresponding pseudo-scalar mediator DM.
The DE model with effective operator $\mathcal{L}_2$ was in close proximity to the ($m_{\tilde{t}} = 1100$ [GeV], $m_{\tilde{\chi}} = 1$ [GeV]) SUSY point on both the high $E_{\mathrm{T}}^{\mathrm{miss}}$ and high $E_{\mathrm{T}}^{\mathrm{miss}} + m_{\mathrm{T}}^{b,\,\mathrm{min}}$ planes.
The 3- and 4-body direct stop models were shown to radiate more than the other models as their $< p_{\mathrm{T}}^{t1,2} >$ was noticeably softer than their $E_{\mathrm{T}}^{\mathrm{miss}}$ as they sat off the diagonal that the other models created. The same was observed for the ($m_{\tilde{t}} = 600$ [GeV], $m_{\tilde{\chi}} = 400$ [GeV]) 2-body decay, and it lay very close to the ($m_{\tilde{t}} = 450$ [GeV], $m_{\tilde{\chi}} = 300$ [GeV]) 3-body decay.

7.1 Next Steps

There are other regions on the $m_{\tilde{t}}$ and $m_{\tilde{\chi}}$ plane that were not included in this study. An immediate goal to improve these planes would be to add the compressed region SUSY to them. Unfortunately for this study there was not enough statistics available to make their inclusion meaningful, but generating them with more events would fix that issue. Any other models that could be added would also be beneficial.

Acknowledgements

There is a huge list of people who helped make my time at DESY incredibly enjoyable and rewarding, and although I am not able to mention everyone; to each I am very grateful.
First, I would like to thank my supervisors Matthias and Krisztian for their incredible support throughout the project, the long physics conversations were greatly appreciated. Also, a special shout out to Xuanhong for putting up with all my questions. Finally, I wish to thank the summer student organisers and the ATLAS group for the educational and truly memorable experience here in Hamburg.

References

[1] Yu. A. Golfand and E. P. Likhtman. Extension of the Algebra of Poincare Group Generators and Violation of p Invariance. *JETP Lett.*, 13:323–326, 1971. [Pisma Zh. Eksp. Teor. Fiz.13,452(1971)].

[2] A. Salam and J. Strathdee. Super-symmetry and non-abelian gauges. *Physics Letters B*, 51(4):353 – 355, 1974.

[3] CMS Collaboration) G. Aad et al. (ATLAS Collaboration. *Phys. Rev. Lett.*, 114, 2015.

[4] Savas Dimopoulos and Howard Georgi. Softly broken supersymmetry and su(5). *Nuclear Physics B*, 193(1):150 – 162, 1981.

[5] Benjamin W. Lee and Steven Weinberg. Cosmological lower bound on heavy-neutrino masses. *Phys. Rev. Lett.*, 39:165–168, Jul 1977.

[6] K. G. Begeman, A. H. Broeils, and R. H. Sanders. Extended rotation curves of spiral galaxies: dark haloes and modified dynamics. *Monthly Notices of the Royal Astronomical Society*, 249(3):523–537, 1991.

[7] Dragan Huterer and Daniel L Shafer. Dark energy two decades after: observables, probes, consistency tests. *Reports on Progress in Physics*, 81(1):016901, 2018.

[8] Adam G. Riess et al. Observational evidence from supernovae for an accelerating universe and a cosmological constant. *The Astronomical Journal*, 116(3):1009, 1998.

[9] S. Perlmutter, The Supernova Cosmology Project, et al. Measurements of and from 42 high-redshift supernovae. *The Astrophysical Journal*, 517(2):565, 1999.

[10] Morad Aaboud et al. Search for dark matter produced in association with bottom or top quarks in $\sqrt{s} = 13$ TeV pp collisions with the ATLAS detector. *Eur. Phys. J.*, C78(1):18, 2018.

[11] Technical Report ATL-PHYS-PUB-2018-008, CERN, Geneva, Jun 2018.

[12] Philippe Brax, Clare Burrage, Christoph Englert, and Michael Spannowsky. Lhc signatures of scalar dark energy. *Phys. Rev. D*, 94:084054, Oct 2016.

[13] John Ellis, J.S. Hagelin, D.V. Nanopoulos, K. Olive, and M. Srednicki. Supersymmetric relics from the big bang. *Nuclear Physics B*, 238(2):453 – 476, 1984.

[14] Morad Aaboud et al. Search for a scalar partner of the top quark in the jets plus missing transverse momentum final state at $\sqrt{s}$=13 TeV with the ATLAS detector. *JHEP*, 12:085, 2017.

[15] John Kenneth Anders. Searches for direct pair production of third generation squarks with the ATLAS detector. Sep 2015.

[16] Ulrich Haisch, Priscilla Pani, and Giacomo Polesello. *Journal of High Energy Physics*, 2017(2):131, Feb 2017.